CDDpress

www.nature.com/cddis

ARTICLE OPEN

Reduced protection of RIPK3-deficient mice against influenza by matrix protein 2 ectodomain targeted active and passive vaccination strategies

Teodora Oltean[1,2], Lorena Itati Ibanez[3,4], Tatyana Divert[1,2], Tine Ysenbaert[3,4], Hannelore Van Eeckhoutte[5], Vera Goossens[6], Michael Schotsaert[3,4], Ken Bracke[5], Bert Schepens[3,4], Jonathan Maelfait[1,2], Nozomi Takahashi[1,2,7], Xavier Saelens[3,4,7] and Peter Vandenabeele[1,2,7]✉

RIPK3 partially protects against disease caused by influenza A virus (IAV) infection in the mouse model. Here, we compared the immune protection of active vaccination with a universal influenza A vaccine candidate based on the matrix protein 2 ectodomain (M2e) and of passive immunization with anti-M2e IgG antibodies in wild type and *Ripk3*$^{-/-}$ mice. We observed that the protection against IAV after active vaccination with M2e viral antigen is lost in *Ripk3*$^{-/-}$ mice. Interestingly, M2e-specific serum IgG levels induced by M2e vaccination were not significantly different between wild type and *Ripk3*$^{-/-}$ vaccinated mice demonstrating that the at least the humoral immune response was not affected by the absence of RIPK3 during active vaccination. Moreover, following IAV challenge, lungs of M2e vaccinated *Ripk3*$^{-/-}$ mice revealed a decreased number of immune cell infiltrates and an increased accumulation of dead cells, suggesting that phagocytosis could be reduced in *Ripk3*$^{-/-}$ mice. However, neither efferocytosis nor antibody-dependent phagocytosis were affected in macrophages isolated from *Ripk3*$^{-/-}$ mice. Likewise following IAV infection of *Ripk3*$^{-/-}$ mice, active vaccination and infection resulted in decreased presence of CD8+ T-cells in the lung. However, it is unclear whether this reflects a deficiency in vaccination or an inability following infection. Finally, passively transferred anti-M2e monoclonal antibodies at higher dose than littermate wild type mice completely protected *Ripk3*$^{-/-}$ mice against an otherwise lethal IAV infection, demonstrating that the increased sensitivity of *Ripk3*$^{-/-}$ mice could be overcome by increased antibodies. Therefore we conclude that passive immunization strategies with monoclonal antibody could be useful for individuals with reduced IAV vaccine efficacy or increased IAV sensitivity, such as may be expected in patients treated with future anti-inflammatory therapeutics for chronic inflammatory diseases such as RIPK inhibitors.

Cell Death and Disease (2022)13:280 ; https://doi.org/10.1038/s41419-022-04710-2

INTRODUCTION

Seasonal human influenza viruses cause acute respiratory infections which affect the entire population and kill up to 650,000 people worldwide each year, and are responsible for substantial public health burden and economic cost [1]. Currently, yearly vaccination is considered the most effective measure to prevent or reduce disease caused by influenza A and B viruses. Seasonal influenza vaccines are mostly based on inactivated influenza viruses and their composition is reevaluated yearly for each hemisphere to follow the antigenic drift of the circulating influenza viruses. Influenza vaccines based on the highly conserved extracellular domain of matrix protein 2 (M2e) of influenza A, have been proposed as possible alternatives for currently licensed influenza vaccines [2, 3]. Immunization of laboratory mice with M2e displayed on a virus-like particle (VLP) protect against a potentially lethal influenza A virus (IAV) challenge [4]. This protection can be transferred by serum, requires a functional Fcγ receptor compartment and is mediated by antibody-dependent cellular phagocytosis [4, 5]. Phase I studies with M2e-based vaccine candidates have been completed, which suggested that such vaccine candidates are safe and immunogenic in healthy volunteers (e.g., NCT00819013) [6]. Whether M2e-based prophylactic vaccination strategies prevent or reduce disease caused by IAV infection in humans remains to be determined. A controlled IAV challenge study in healthy volunteers revealed that a dose of 40 mg/kg of a human anti-M2e IgG1 monoclonal antibody was associated with a significant reduction in the total influenza symptom score compared to the placebo treated group [7]. To date, preclinical and clinical M2e-based influenza A vaccine development efforts are continuously being explored [8].

Cell death signaling pathways contribute to the innate immune defense against infectious diseases. One key player in some of

[1]VIB-UGent, Center for Inflammation Research (IRC), Ghent, Belgium. [2]Department of Biomedical Molecular Biology (DBMB), Ghent, Belgium. [3]VIB-UGent Center for Medical Biotechnology, VIB, Ghent, Belgium. [4]Department of Biochemistry and Microbiology, Ghent University, Ghent, Belgium. [5]Laboratory for Translational Research in Obstructive Pulmonary Diseases, Dept of Respiratory Medicine, Ghent University Hospital, Ghent, Belgium. [6]VIB Screening Core & UGent Expertise Centre for Bioassay Development and Screening (C-BIOS), Ghent, Belgium. [7]These authors contributed equally: Nozomi Takahashi, Xavier Saelens, Peter Vandenabeele. ✉email: Peter.Vandenabeele@irc.vib-ugent.be
Edited by Professor Gerry Melino

Received: 6 September 2021 Revised: 16 February 2022 Accepted: 3 March 2022
Published online: 29 March 2022

these pathways is Receptor-Interacting serine/threonine-Protein Kinase 3 (RIPK3) [9]. Indeed, RIPK3 is involved in the protection against IAV infection by several mechanisms [10–14]. RIPK3 kinase activity, for example, is implicated in TNF-and ZBP1-mediated necroptosis, while as a scaffold it is implicated in apoptosis upon IAV infection [14]. Beyond its involvement in the protection against IAV infection, the contribution of RIPK3 to vaccine-induced immune protection conferred by active vaccination strategies has not been addressed. In this study, we compared the immunogenicity of active vaccination with M2e-VLPs and the protective potential of passive transfer of M2e-specific IgG monoclonal antibodies in wild type and *Ripk3*-deficient mice against an IAV challenge.

RESULTS

RIPK3 is required for protection against IAV following active vaccination with M2e-VLP

To evaluate if active vaccination remains effective in a host that is susceptible to IAV infection, we immunized *Ripk3*$^{-/-}$ mice with a broad-spectrum influenza A vaccine candidate based on M2e, and subsequently challenged these mice with a lethal dose of IAV (Fig. 1). The *Ripk3*$^{-/-}$ mice and their *Ripk3*$^{+/+}$ littermates were primed and immunized with the M2e-VLP vaccines or with phosphate-buffered saline (PBS), as a negative control. As expected at this high IAV challenge dose, there is no difference between unvaccinated *Ripk3*$^{-/-}$ versus *Ripk3*$^{+/+}$ mice [14]. Almost all *Ripk3*$^{-/-}$ mice, though vaccinated died soon after infection (Fig. 1A and Supplementary Fig. 2A), while most *Ripk3*$^{+/+}$ littermates survived. This indicates that RIPK3 not only is involved in the protection against IAV infection [14, 15], but is also crucial for the efficacy of vaccination against IAV.

Both the innate and acquired immune responses are required for an effective immune response post active vaccination [16]. Therefore, we checked whether the absence of protection of RIPK3-deficient mice following vaccination would be due to impaired production of specific anti-M2e antibodies (Fig. 1B). Remarkably, sera taken from *Ripk3*$^{-/-}$ mice isolated 2 weeks after the boost with M2e-VLP revealed similar levels of M2e-specific IgG antibodies as the *Ripk3*$^{+/+}$ littermates. This finding suggests that besides the antibody production post immunization, other mechanisms contribute to effective vaccination which would be lacking in RIPK3-deficient mice. Active vaccination with M2e-VLP decreases viral titers in the lungs upon IAV challenge [4]. Since RIPK3 is important for viral protection we examined whether viral titers would be different in vaccinated *Ripk3*-deficient and—proficient animals. At day 6 post-infection, we measured viral titers in the lungs of non-vaccinated and vaccinated mice. We observed that in non-vaccinated mice, the viral loads were similar between the *Ripk3*$^{+/+}$ and the *Ripk3*$^{-/-}$ mice. However, both in *Ripk3*$^{+/+}$ and *Ripk3*$^{-/-}$ mice vaccination reduces the viral load, however, this tendency is less outspoken in *Ripk3*$^{-/-}$ (from mean 1.1×10^7 to mean 6.9×10^6, or a reduction of about 40%) compared to the *Ripk3*$^{+/+}$ mice (from mean 1.34×10^7 to mean 2×10^6, or a reduction of about 90%) (Fig. 1C). These data suggest that the lack of protection after vaccination in *Ripk3*$^{-/-}$ mice might be due to increased virus loads in the lungs as a consequence of decreased vaccination efficacy or increased IAV sensitivity and virus propagation.

IAV-associated inflammation is reduced in vaccinated *Ripk3*$^{-/-}$ mice

In order to understand the underlying phenomena explaining the difference in vaccination efficiency in *Ripk3*$^{-/-}$ and *Ripk3*$^{+/+}$ mice, we determined immune cells infiltration in the lungs following vaccination and infection. Indeed immune cell infiltration is required for protection against IAV lethal infection [17]. We observed that the lung inflammation score of non-vaccinated and vaccinated *Ripk3*$^{-/-}$ showed a similar tendency for reduced inflammation by histology and injury score (Fig. 2A), less immune infiltrates (Supplementary Fig. 1A) and a higher amount of dead cell as detected by TUNEL staining compared to littermate controls (Fig. 2B). However, quantification of these parameters did not reveal significance because only discrete areas are affected (Fig. 2D and Supplementary Fig. 1B). It was previously shown that IAV-specific CD8+ T cell numbers were significantly diminished upon infection in *Ripk3*$^{-/-}$ mice compared to littermate controls [10]. These CD8+ T are important for the support and efficient effector immune response. Here, we also observed that in the lung the number of CD8+ cells was more pronouncedly decreased in the vaccinated *Ripk3*$^{-/-}$ mice compared to the vaccinated *Ripk3*$^{+/+}$ littermates (Fig. 2C, D). All these observations suggest that the *Ripk3*$^{-/-}$ mice may have an impaired innate immune response against IAV leading to reduced protection or enhanced sensitivity.

One possibility is that RIPK3 might be implicated in immune cell infiltration and removal of dead cell corpses reflecting a possible deficit in the capacity of executing efferocytosis and antibody-dependent cellular phagocytosis due to reduced recruitment of phagocytes or reduced phagocytic efficacy, or a combination of both. However, *Ripk3*-deficient peritoneal and alveolar macrophages are as competent as littermate control to perform efferocytosis and antibody-dependent phagocytosis, respectively. Indeed, we found that RIPK3 deficiency does not affect the capacity of peritoneal macrophages to engulf dexamethasone-treated apoptotic thymocytes (Fig. 3A). Since Fc receptors and alveolar macrophages have been demonstrated to be crucial for the protection against lethal IAV infection by passive transfer of anti-M2e IgG [5], we also examined a possible impairment of the process of antibody-dependent cellular phagocytosis (ADCP). To this end, we developed a method in which M2e-coated polystyrene beads mimicking infected cells were incubated with primary alveolar macrophages isolated from *Ripk3*$^{+/+}$ or *Ripk3*$^{-/-}$ mice in the presence or absence of M2e-specific antibodies. We observed that *Ripk3* deficiency does not affect the capacity of alveolar macrophages to engulf M2e-coated beads with or without antibodies, demonstrating that RIPK3 is also dispensable for ADCP (Fig. 3B). Therefore we conclude that very likely the reduced recruitment of immune cells combined with the enhanced sensitivity of RIPK3-deficient mice for IAV infection [10–14] may explain the observed reduced survival of *Ripk3*$^{-/-}$ mice following vaccination.

Increased doses of passive immunization with Anti-M2e monoclonal antibodies can completely protect *Ripk3*-deficient mice

Passive transfer of anti-M2e monoclonal antibodies protects mice against IAV infection [18]. We wondered whether the increased sensitivity to IAV lethality in *Ripk3*-deficient mice could be rescued by passive transfer of anti-M2e monoclonal antibodies providing a protective alternative for inefficient active immunization in *Ripk3*$^{-/-}$ mice. In case of a lethal dose of IAV infection (5× LD_{50}), wild type littermates were completely protected by passive transfer of a moderate dose of anti-M2e antibodies (10 µg/20 g or 0.5 mg/kg), while almost half of the *Ripk3*$^{-/-}$ mice succumbed (Fig. 4A and Supplementary Fig. 2B). Cox regression did not reveal any significant difference ($p = 0.517$) between female and male mice exhibiting partial protection in *Ripk3*$^{-/-}$ during passive vaccination. However, when higher amounts of anti-M2e monoclonal antibodies (50 µg/20 g or 2.5 mg/kg) were used in the passive transfer in combination with the same viral dose for challenge (5× LD_{50}), then all *Ripk3*$^{-/-}$ mice were also completely protected (Fig. 4B and Supplementary Fig. 2C). If mice were infected with a lower viral dose (here 2.4× LD_{50}) in combination with the standard dose of anti-M2e (10 µg/20 g or 0.5 mg/kg) we also reached complete protection in *Ripk3*$^{-/-}$ mice (Fig. 4B and Supplementary Fig. 2C). Altogether these passive vaccination results in conditions of decreased anti-viral protection show a balance between the capacity of passively transfer M2e antibodies to cope with

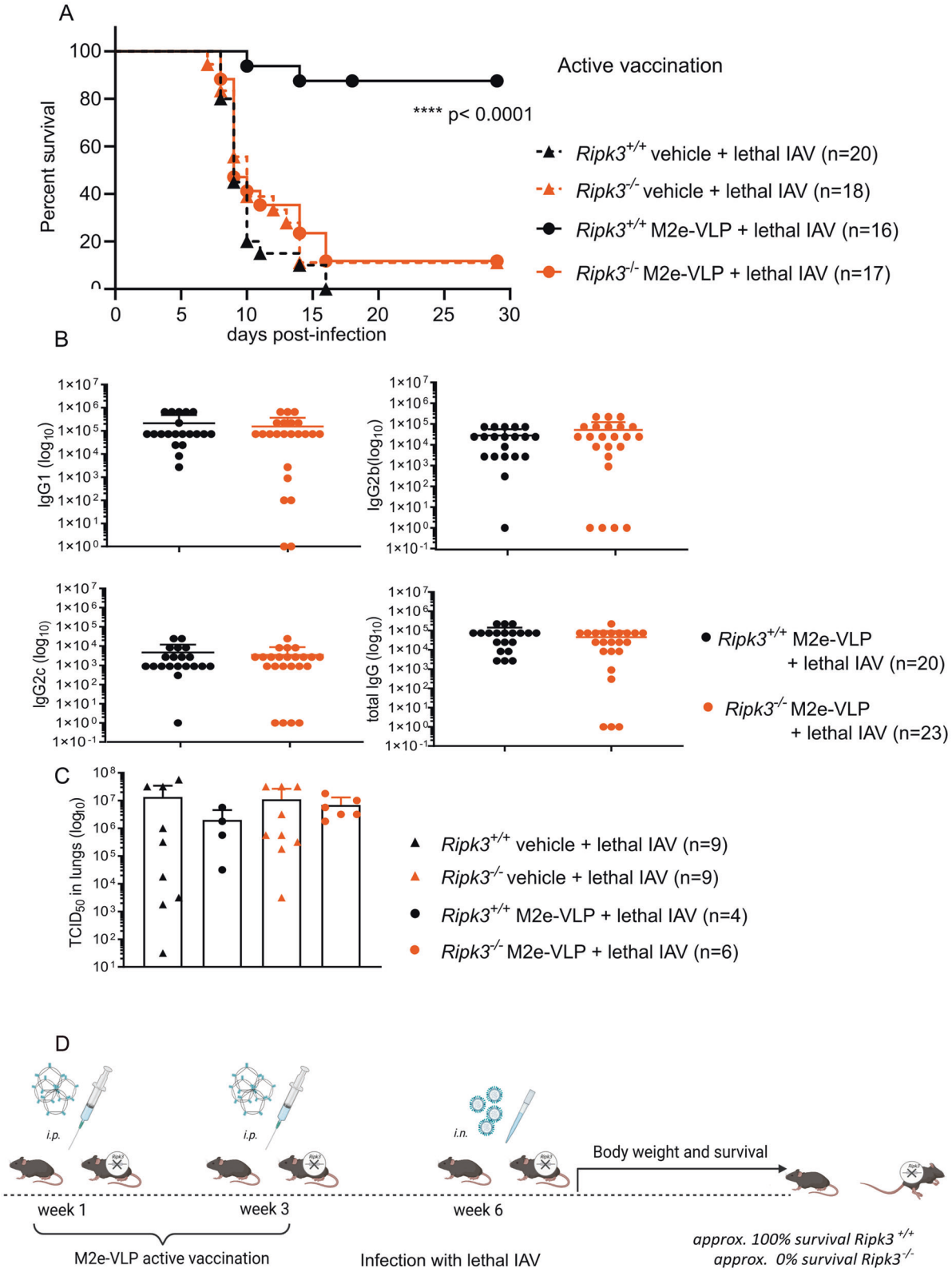

infection and the dose of infection (Fig. 4C). This demonstrates that a deficiency in an antiviral response gene such as *Ripk3* could be compensated by sufficient levels of passively administered monoclonal antibodies.

DISCUSSION

In this study, we examined whether a state of fairly enhanced sensitivity to IAV infection in *Ripk3*$^{-/-}$ mice [14], would affect the efficacy of active immunization with M2e viral antigen or passive

Fig. 1 Ripk3-deficient mice are not protected against IAV lethal infection following active vaccination with M2e-VLP despite similar serum levels of M2e-specific antibodies and viral clearance. A Active vaccination with M2e-VLP particles was administered with Alhydrogel® adjuvant intraperitoneally. Age-matched *Ripk3*$^{+/+}$ and *Ripk3*$^{-/-}$ mice received either 5 µg/mouse M2e-VLP with Alhydrogel® adjuvant vaccination or just the Alhydrogel® adjuvant dissolved in PBS (vehicle) 3 weeks and 6 weeks before infection. Lethal challenge was done with the mouse-adapted influenza X47 with either 2 × LD_{50} (virus batch 1) or 0.5 × LD_{50} (virus batch 2). The experiment was repeated four times independently and data were pooled. Survival curves were plotted for indicated groups and evaluated statistically according to Kaplan–Meier. A log-rank test verified significant differences between *Ripk3*$^{+/+}$ and *Ripk3*$^{-/-}$ mice post-vaccination; ****p-value< 0.0001 (GraphPad Prism 8). Similar numbers of female and male mice were used comparing both genotypes (19 females, 3 males *Ripk3*$^{+/+}$ versus 21 females, 6 males *Ripk3*$^{-/-}$). The body weight readout of this experiment is provided in Supplementary Fig. 2A. **B** RIPK3-deficient mice effectively produce specific antibodies against M2e: Age-matched *Ripk3*$^{+/+}$ and *Ripk3*$^{-/-}$ mice were primed (6 weeks before infection) then immunized (3 weeks before infection) 10 µg M2e-VLP with Alhydrogel® adjuvant or received PBS with Alhydrogel® adjuvant (vehicle). Serum samples were prepared two weeks after each immunization. Titers of IgG1 IgG2a IgG2b and total IgG against M2e were measured after the immunization were determined by ELISA. The legend shows the M2e-specific antibody titers obtained for individual mice (dots) of each group from three independent experiments. **C** Virus clearance from the lungs post vaccination is independent from RIPK3-deficiency: On day 6 post-infection, lungs were harvested and lung homogenates were assessed for viral titers by $TCID_{50}$. Data for pooled lung homogenates from different mice (two independent experiments) of the same group are shown. The means for $TCID_{50}$ are shown for each group as indicated in the legend. Error bars represent SD. **D** Overview of the active vaccination strategy and the results obtained in *Ripk3*$^{+/+}$ and *Ripk3*$^{-/-}$ mice.

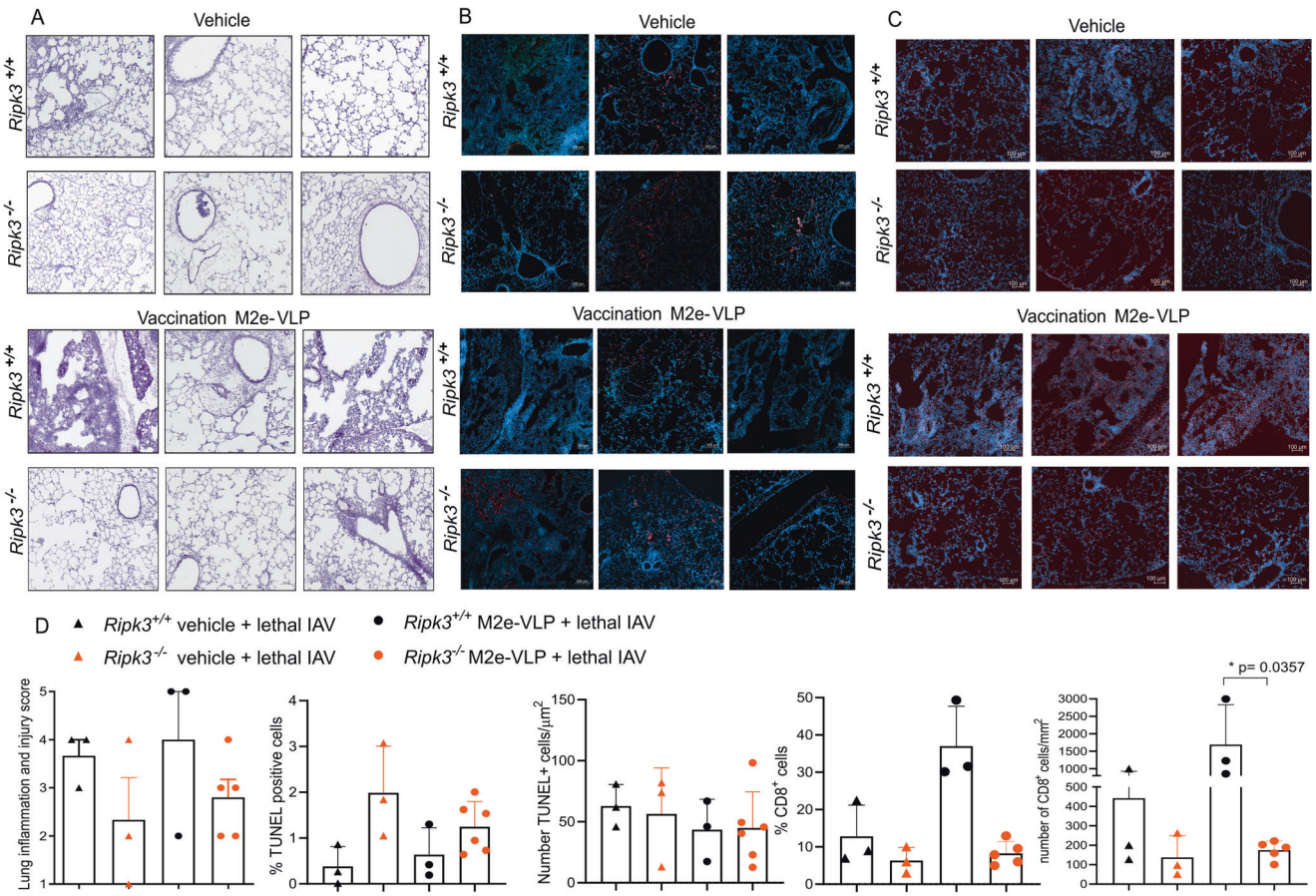

Fig. 2 Immune cells infiltration in the lungs is required for protection against IAV lethal infection. A Vaccinated and non-vaccinated *Ripk3*$^{+/+}$ and *Ripk3*$^{-/-}$ mice challenged with lethal IAV dose challenge (2 × LD_{50}; virus batch 1) were sacrificed at 6 days post-infection and their lungs were collected and stained with hematoxylin-eosin. Representative images of individual mice revealed less inflammation in the vaccinated *Ripk3*$^{-/-}$ mice compared to their *Ripk3*$^{+/+}$ control. **B** Vaccinated and non-vaccinated *Ripk3*$^{+/+}$ and *Ripk3*$^{-/-}$ mice challenged with lethal IAV were sacrificed at 6 days post-infection and their lungs were collected. **C** Representative images displaying TUNEL positivity (red) and cells nuclei (blue) are shown in (**B**) and CD8 positivity (red) and cell nuclei (blue) is shown in (**C**). A tendency to accumulate more dying-cells in the lungs of *Ripk3*$^{-/-}$ mice compared to their *Ripk3*$^{+/+}$ controls is observed. **D** The extent of lung inflammation and injury score was blindly scored (0 - no inflammatory cell infiltration; normal alveolar septa; 1 - mild peribronchial/perivascular inflammatory cell infiltration in parts of the lung; normal alveolar septa; 2 - moderate peribronchial/perivascular inflammatory cell infiltration in parts of the lung; mild thickening of alveolar septa; 3 - severe alveolar and interstitial inflammatory cell infiltration in parts of the lung; moderate thickening of alveolar septa; 4 - very severe alveolar and interstitial inflammatory cell infiltration in parts of the lung; severe thickening of alveolar septa; 5 - very severe alveolar and interstitial inflammatory cell infiltration throughout the lung; severe thickening of alveolar septa). TUNEL positivity and for CD8 positivity was scored with a software 0.2.3. and QuPath software 0.3.0. respectively. Graphics and statistical analysis were done with GraphPad Prism 8. Comparisons were done with Mann–Whitney test in GraphPad Prism 8.

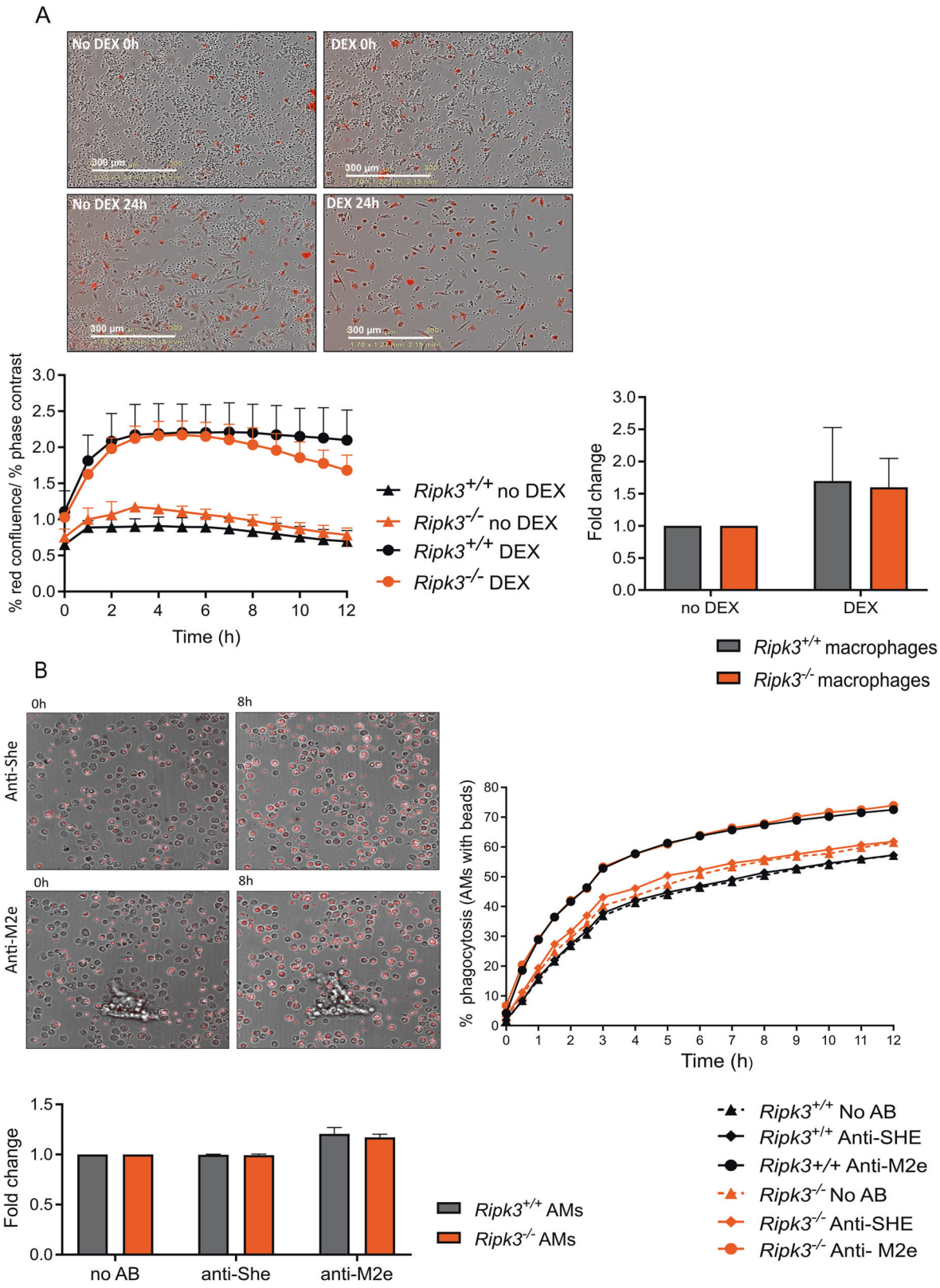

immunization by transfer of anti-M2e monoclonal antibodies. Since RIPK3, both as a kinase and a scaffold protein, is implicated in many cellular processes such as necroptosis, apoptosis, inflammasome activation, and pyroptosis induction, its loss may be associated with a reduced induction of an anti-viral state in an infected host. This could be a model for populations at risk for severe IAV infection such as elderly, children, pregnant women, and immunodeficient patients [19, 20]. To date, a potential

Fig. 3 RIPK3-deficient macrophages are competent to perform efferocytosis and antibody-dependent cellular phagocytosis. A Primary peritoneal macrophages isolated from *Ripk3*$^{+/+}$ and *Ripk3*$^{-/-}$ mice were co-incubated in 1:5 ratio with apoptotic (dexamethasone-killed, DEX) or non-apoptotic (no DEX) thymocytes stained with pH-sensitive dye, CypHER 5E. Live cell imaging was performed with IncuCyte® S3 (Sartorius). Representative images of macrophages which engulfed DEX-treated or no DEX-treated thymocytes become positive for CypHER 5E (red) can be seen. The difference between *Ripk3*$^{+/+}$ and *Ripk3*$^{-/-}$ at 8 h of co-incubation is shown as fold change relative to the no DEX control (three independent experiments). **B** M2e-coated fluorescent polystyrene beads were incubated in 2.5:1 ratio with primary alveolar macrophages isolated form *Ripk3*$^{+/+}$ or *Ripk3*$^{-/-}$ mice in the absence or presence of 0.1 μg/mL of isotype control antibody, Anti-SHE or an anti-M2e mouse IgG2a monoclonal antibody (Mab65) specific antibody, Anti-M2e. Live cell imaging was performed with Operetta high content imaging system and analysis was done with Harmony software. The difference between *Ripk3*$^{+/+}$ and *Ripk3*$^{-/-}$ at 8 h of co-incubation is shown as fold increase in antibody-mediated phagocytosis relative to no antibody control (three independent experiments). Significance was determined using one-way ANOVA with Tukey correction (GraphPad Prism 8). Error bars represent SEM.

correlation between RIPK3 single nucleotide polymorphism (SNPs) and an increased susceptibility to IAV in human hosts has not been investigated. Additional investigation needs to be done to explore this possibility. Given the development of RIPK1 and RIPK3 inhibitors as anti-inflammatory treatments for chronic inflammatory diseases [21–23], our work reveals an important caveat. Future patients receiving such RIPK inhibitors may be immunocompromised and could benefit from monoclonal antibody therapy overcoming any deficits in influenza immunity. We and others showed that, at least in mice, RIPK3 is an important mediator of protection against IAV infection [10, 14, 15, 24–26]. However, we have reported previously that this sensitizing effect of RIPK3 deficiency is only limited to a certain level of viral challenge. Indeed, morbidity and lethality after a high IAV challenge *Ripk3*$^{-/-}$ mice were comparable to those in their *Ripk3*$^{+/+}$ littermates [14].

Interestingly, active immunization of *Ripk3*$^{-/-}$ mice with recombinant M2e-VLPs could raise equal titers of M2e-specific serum IgG antibodies as compared to immunization of *Ripk3*$^{+/+}$ mice, but this apparently does not result in a protective effect against a lethal influenza challenge. The full ability of *Ripk3*$^{-/-}$ mice to produce antibodies against M2e suggests that other factors than M2e-specific antibodies contribute to an efficient antibody-mediated protection. We found that non-vaccinated and vaccinated *Ripk3*$^{-/-}$ mice display reduced immune cells infiltration in the lungs and accumulate more dying cells post infection compared to their wild type littermates. Conceptually, these phenomena could be due to decreased ADCP and efferocytosis. However, our experiments did not reveal a difference in these processes in peritoneal and alveolar-derived macrophages from *Ripk3*$^{+/+}$ littermates and *Ripk3*$^{-/-}$ mice. Since the *Ripk3*$^{-/-}$ mice are able to produce normal levels of M2e-specific antibodies following M2e-VLP immunization, humoral immune responses following active immunization are not impaired in *Ripk3*-deficient mice. However, despite these equal levels of protective antibodies, a differential response was observed following viral challenge between *Ripk3*$^{-/-}$ mice and *Ripk3*$^{+/+}$ littermates. The former showed a tendency for increased viral loads following vaccination, decreased inflammation score, reduced infiltration of CD8+ immune cells, and accumulation of dead cell corpses in the lungs, suggesting that the innate arm is compromised in *Ripk3*-deficient mice. We do not exclude that other immune cells important in the IAV clearance such as neutrophils and NK cells could also be reduced in the vaccinated *Ripk3*$^{-/-}$ mice contributing to their inability to efficiently respond to active vaccination.

Although most of the differences in viral load, inflammation, and cell death parameters in the lung between the vaccinated *Ripk3*$^{+/+}$ *and Ripk3*$^{-/-}$ mice only showed a tendency and were not significant, the combination of these three parameters can have a crucial impact on the lethal phenotype observed in *Ripk3*$^{-/-}$ mice despite vaccination. Also, we cannot exclude that there might be a difference in the induction of M2e-specific T cells [25]. Altogether, our work supports two potential, non-exclusive scenarios for the enhanced sensitivity of *Ripk3*$^{-/-}$ mice in the active vaccination model. One possibility is that non-humoral arms of vaccine-induced immunity are impaired under RIPK3 deficiency leading to reduced numbers of CD8+ T-cells. The other possibility reflects a cell-autonomous role of RIPK3 in controlling IAV infection up to mid-range IAV doses. In order to examine whether the immunocompromised *Ripk3*-deficient mice could still be protected by antibodies, we delivered anti-M2e monoclonal antibodies prior to IAV infection. The transfer of high dose of anti-M2e monoclonal antibodies protects the *Ripk3*$^{-/-}$ mice from a lethal IAV infection [18] while a moderate dose does not. Passive transfer with anti-M2e monoclonal antibodies was shown to limit viral load in the infected lungs which can modulate the susceptibility of the *Ripk3*$^{-/-}$ mice to the IAV making them less susceptible to the same dose of infection [14, 26]'. It is clear from our experiments that modulation of the viral dose in the lungs is crucial for the survival of *Ripk3*$^{-/-}$ mice [14]. Protective host strategies against IAV infection consist in the capacity to rapidly recognize and eliminate the virus or to quickly regain fitness by reducing the negative impact of infection [27]. It seems that *Ripk3*$^{-/-}$ mice are not able to reduce the pathogen burden when it reaches a certain threshold, and eventually succumb to the infection [14]. Interestingly, active vaccination helps them to produce antibodies, but not to sufficiently to reduce viral titers, therefore *Ripk3*$^{-/-}$ mice, are not protected by this vaccination. However, when passive immunization is used at a high dose, this could decrease viral burden and rescue the *Ripk3*$^{-/-}$ mice from lethal IAV infection.

The reduced infiltration of immune cells and CD8+ cells observed in *Ripk3*$^{-/-}$ mice may also be explained, at least partly, by reduced vascular permeability. Indeed, *Ripk3*$^{-/-}$ mice have reduced endothelial permeability affecting tumor migration into the lung using a B16 melanoma model [28]. It is therefore conceivable that a similar endothelial mechanism may also contribute to reduced diffusion of antibodies in lung tissue and BAL fluid, in line with the reduced efficacy of humoral protection despite identical titers following active vaccination and with the higher amount of monoclonal antibodies required for protection following passive vaccination. To examine such a role of RIPK3 in the endothelial compartment during active and passive vaccination, one would need to perform experiments in endothelium-specific *Ripk3*$^{-/-}$ mice.

This finding provides a clinically relevant option for patients at risk which may not respond to active vaccination and argues that in antiviral compromised organisms the passive vaccination may bypass the affected innate immune system. For example, one study on adults hospitalized with acute respiratory illness during the 2017–18 influenza season in the USA showed that the deduced influenza vaccine effectiveness in hospitalized immunocompromised patients was as low as 5% compared to 41% in the immunocompetent individuals [28]. Furthermore, emerging data show that monoclonal antibodies are promising candidates for the treatment of IAV infections in the future [29, 30], whenever vaccines are not effective. Some of these antibodies are currently being evaluated in clinical trials [31]. These monoclonal antibody-based anti-IAV strategies may also be required to cope with the actual COVID-19 pandemic and the continuous occurrence of variants.

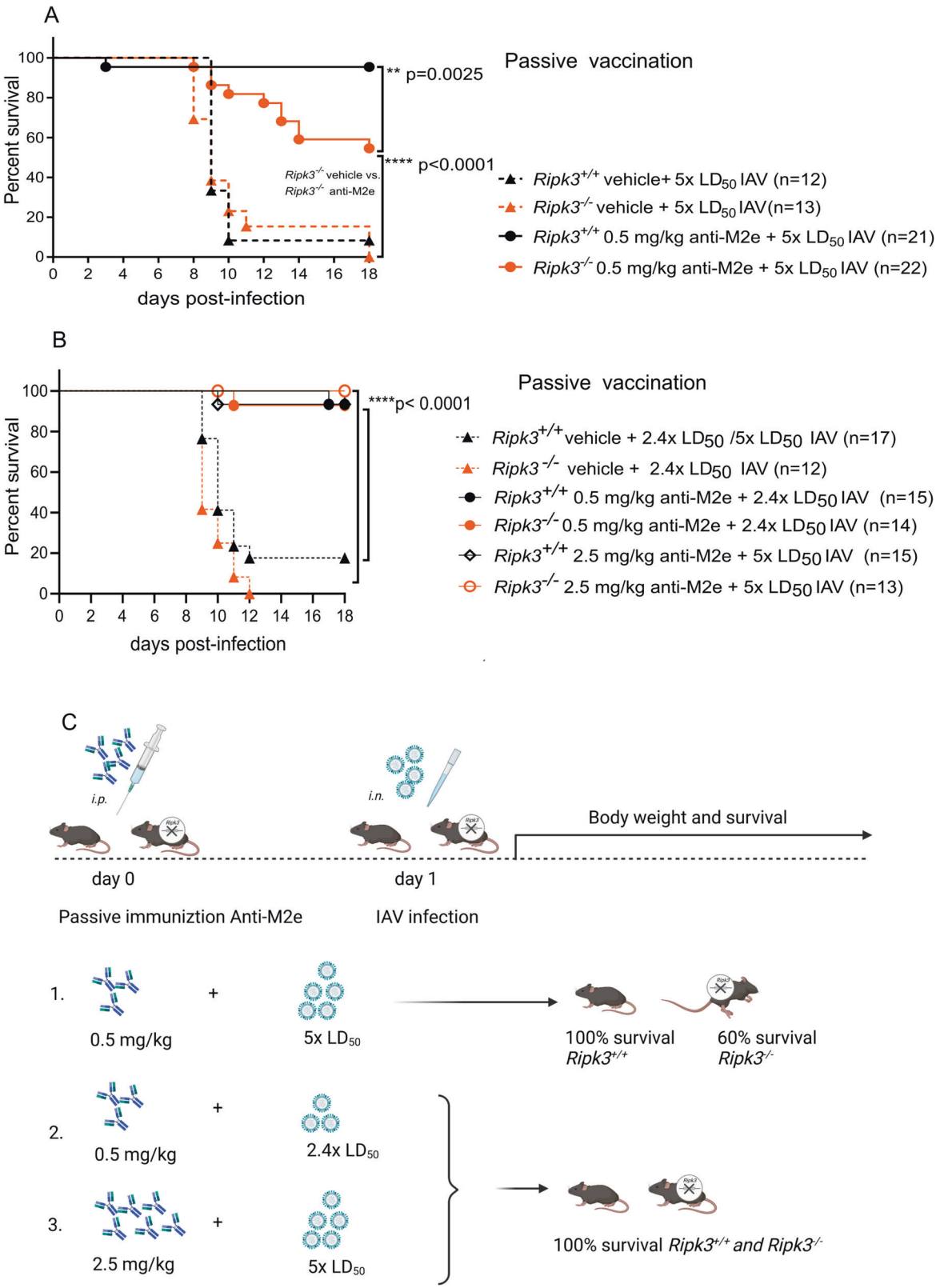

MATERIAL AND METHODS

Mice

Ripk3$^{-/-}$ and littermate controls *Ripk3*$^{+/+}$ were kindly provided by Vishva Dixit (Genentech, San Francisco). The *Ripk3*$^{-/-}$ animals were congenic to the C57BL/6N background. All mice were housed in individually ventilated cages in a conventional animal house. 7–13 weeks-old mice were used in all experiments. All animal experiments were performed under conditions specified by law (European Directive and Belgian Royal Decree of November 14, 1993) and reviewed and approved by the Institutional Ethics Committee on Experimental Animals (EC2016-17).

Fig. 4 Increased doses of passive immunization with Anti-M2e monoclonal antibodies can completely protect *Ripk3*-deficient mice. A The administration of a standard dose Anti-M2e (0.5 mg/kg) and challenge with lethal IAV (5 × LD_{50}; viral batch 3) (four independent experiments, total number of mice indicated between brackets). The passive immunization with monoclonal Anti-M2e was done i.p. one day before the i.n. infection with IAV. Survival was monitored daily for up to 18 days post-challenge. Survival curves were plotted for indicated groups and evaluated statistically according to Kaplan–Meier (GraphPad Prism 8). Similar numbers of female and male mice were used comparing both genotypes (18 females, 15 males *Ripk3*$^{+/+}$ versus 18 females, 17 males *Ripk3*$^{-/-}$). The body weight readout of this experiment is provided in Supplementary Fig. 2B. Cox regression did not reveal any significant difference ($p = 0.517$) in survival between female and male mice. **B** The combination of passive immunization with a standard Anti-M2e dose (0.5 mg/kg) and a decreased (but still lethal) IAV dose (2.4 × LD_{50}; viral batch 3) was performed three times (total number of mice indicated between brackets). The combination of passive immunization with an increased dose of Anti-M2e (2.5 mg/kg) and lethal IAV dose (5 × LD_{50}; viral batch 3) in three independent experiments (total number of mice indicated in the legends). The passive immunization with monoclonal Anti-M2e was done i.p. one day before the i.n. infection with IAV. Survival was monitored daily for up to 18 days post-challenge. Survival curves were plotted for indicated groups and evaluated statistically according to Kaplan–Meier (GraphPad Prism 8). The body weight readout of this experiment is provided in Supplementary Fig. 2C. **C** Scheme of passive immunization and main conclusions. Overview of the results in terms or survival of *Ripk3*$^{+/+}$ and *Ripk3*$^{-/-}$ mice are shown in approximative percentages based on the results in panels (**A** and **B**). Similar numbers of female and male mice were used comparing both genotypes (27 females, 14 males *Ripk3*$^{+/+}$ versus 26 females, 13 males *Ripk3*$^{-/-}$).

Active vaccination with M2e-VLP and virus challenge

Age-matched *Ripk3*$^{+/+}$ and *Ripk3*$^{-/-}$ mice were intraperitoneally injected two times with 5 µg of purified M2e-VLP in the absence or presence of Alhydrogel® adjuvant (Brenntag Biosector Specification, total volume, 200 µl). The M2e-VLP 1965, expressed by and purified from recombinant *E. coli* cells, was used for active vaccination and comprises 1–162 amino acids of HBc and they are able to entrap bacterial RNA [31]. Control mice received a vehicle containing Alhydrogel® adjuvant in PBS, pH 7.4. The two injections were given at 3-week intervals. Three weeks after the last immunization, mice were challenged with a lethal dose of mouse-adapted of X47 influenza virus. Depending on the viral batch preparation the challenge following active vaccination was with a lethal dose of either 2 × LD_{50} [1 × LD_{50} corresponding to approximately 30 tissue culture infectious dose 50 ($TCID_{50}$)] (virus batch 1) or 0.5 × LD_{50} (1 × LD_{50} corresponds with 80 plaque-forming units or pfu) (virus batch 2). The virus was administered intranasally in a total volume of 50 µl to mice anesthetized by ketamine (44 mg/kg) and xylazine (5 mg/kg). Mice were either monitored for survival and weight loss over a period of 18 days. We used the following 4 scores of clinical symptoms: 0 = no visible signs of disease; 1 = slight ruffling of fur; 2 = ruffled fur, reduced mobility; 3 = ruffled fur, reduced mobility, rapid breathing; 4 = ruffled fur, minimal mobility, huddled appearance, rapid and/or labored breathing indicative of pneumonia and body temperature below 32 °C. For the combination of body weight loss by 30% and a clinical score 4 the mice were considered moribund and euthanized by CO_2 asphyxiation or cervical dislocation (EC2016-17).

Serum preparation and analysis of the production of antibodies against M2e

Blood samples were obtained from every mouse, before immunization, after the first boost, and after the second boost. Serum was prepared and the presence of M2e-specific antibodies was determined by ELISA, as described previously [4].

Passive transfer of Anti-M2e monoclonal antibodies and virus challenge

Purified Anti-M2e IgG monoclonal antibody (clone mAb 65) [18] or isotype control were i.p. injected at 0.5 mg/kg or 2.5 mg/kg as indicated in the figure legends (200 µl/mouse) in naive mice. After 24 h, the mice were anesthetized with a mixture of ketamine (44 mg/kg) and xylazine (5 mg/kg) and challenged by intranasal administration of 50 µl of different doses of mouse-adapted X47 (H3N2) IAV, as indicated in the figure legends. For passive immunization experiments challenges were performed with lethal doses of 2.4 × LD_{50} or 5 × LD_{50} of a viral batch in which 1 × LD_{50} corresponds to 175 pfu (virus batch 3). Mortality and body weight loss were monitored for up to 30 days after challenge.

$TCID_{50}$ assay

$TCID_{50}$ assays were used to determine the amount of infectious virus in lung homogenates of each condition. MDCK cells cultured in Dulbecco's modified Eagle's medium (DMEM) supplemented with 10% FCS, non-essential amino acids, 2 mM L-glutamine, and 0.4 mM Na-pyruvate were seeded in 96-well plates to reach confluence overnight at 37 °C in 5% CO_2. The cells were washed in serum-free medium and incubated with 10-fold dilutions of virus samples containing 1 µg/ml of TPCK-treated trypsin (Sigma). After 6 days, the presence of virus in each well was determined by agglutination of chicken erythrocytes. $TCID_{50}$ values were calculated based on the Reed and Muench method [32].

Lung histology

Lungs were collected from indicated mice sacrificed on day 6 post-infection. Tissues were covered in cryo-embedding media, kept in liquid nitrogen until completely submerged, then stored at −80 °C until ready for sectioning. 4 mm sections were cut with a cryotome and stained with haematoxylin and eosin. For immunofluorescence, sections were fixed in 4% paraformaldehyde for 1 h at RT, washed with PBS, then incubated in "permeabilisation solution" containing 0.05% TX-100 and 0.1% sodium citrate for 2 min on ice (4 °C). Cell death was analyzed with an in situ cell death detection kit (TMR-red, Roche) after antigen retrieval either alone or followed by staining with anti-CD45 (AB 10558 Abcam) and Goat anti-Rabbit IgG DyLight488 (ThermoFicher ref: 35553). Anti-CD8a (AB 217344, Abcam) was used 1/100 combined with a secondary Goat anti-Rabbit IgG AF568. Hoechst 33342 was used to stain nuclei. Brightfield and fluorescence microscopy was performed using ZEISS Axio Scan.Z1. Samples were analyzed with Zen 3.2. blue edition (Zeiss) and quantified with QuPath software 0.2.3.

Macrophage isolation

Resident peritoneal macrophages were obtained by flushing the peritoneal cavity of mice with 10 ml of cold PBS containing 5% FCS. Collected cells were spun down and resuspended in RPMI 1640 medium supplemented with 10% FCS, 10 mM Na-pyruvate, L-glutamine, penicilin/strepomycin (100 U/100 Ag/ml), HEPES, β-mercaptoethanol, and 100 mM non-essential amino acids. The cells were plated at a concentration of 4.5×10^5 cells per well in a 24-well plate and maintained at 37 °C in a 5% CO_2 humidified atmosphere. Floating cells were washed away the next day and remaining peritoneal macrophages were used 2 days after isolation. Alveolar macrophages were collected from mice were anesthetized via intraperitoneal injection of Nembutal (pentobarbital; 125 mg/kg in PBS; Lundbeck, Valby, Denmark). A small incision was made in the trachea to put a lavage cannula in the trachea. Lungs were lavaged three times with 1 ml of HBSS with 0.05 mM EDTA (Sigma-Aldrich) and the bronchoalveolar lavage fluid (BALF) was kept on ice. Collected cells were centrifuged, resuspended in RPMI 1640 medium supplemented with 10% FCS, 10 mM Na-pyruvate, L-glutamine, penicillin/streptomycin (100 U/100 Ag/ml), HEPES, β-mercaptoethanol, and seeded at 1×10^5 cells per well in a 96-well plate. Cells were allowed to adhere at 37 °C in a 5% CO_2 humidified atmosphere for 2 h before phagocytosis assays.

Beads preparation and ADCP

Amine-modified polystyrene beads (Polysciences) were pre-activated with 8% (vol/vol) glutaraldehyde for 4 h at room temperature. Beads were conjugated with 10 µg/ml of M2e peptide and 0.2 mg/ml of Alexa Fluor N-hydroxy-succinimide ester dyes (Life Technologies) on a rotating wheel overnight at 4 °C. After quenching in PBS containing 0.5 M glycine for 2 h, beads were used for ADCP assays. Beads were incubated in 2.5:1 ratio with freshly isolated alveolar macrophages in the absence or presence of 0.1 µg/ml of isotype control antibody, anti-SHE (IgG2a isotype control MAbs directed against the small hydrophobic protein of human respiratory

syncytial virus) [33] or M2e-specific antibody [34, 35]. Live cell imaging was performed with Operetta high content imaging system and analysis was done with Harmony software (PerkinElmer).

Efferocytosis assay

Thymocytes were isolated from 4 to 6-week-old mice and induced to undergo apoptosis with 20 μM dexamethasone for 4 h at 37 °C in 5% CO_2 incubator. Thymocytes were then stained with CypHer5E (GE Healthcare), counted, and added to adherent peritoneal macrophages at a macrophage: apoptotic target ratio of 1:5. Live cell imaging was performed and analyzed with IncuCyte® S3 (Sartorius).

DATA AVAILABILITY

The datasets used and/or analyzed during the current study are available from the corresponding author on reasonable request.

REFERENCES

1. Angiolella LSD, Lafranconi A, Cortesi PA, Rota S, Cesana G, Mantovani LG. Costs and effectiveness of influenza vaccination: A systematic review. Ann Ist Super Sanità. 2018;54:49–57.
2. Kim MC, Lee JS, Kwon YM, O E, Lee YJ, Choi JG, et al. Multiple heterologous M2 extracellular domains presented on virus-like particles confer broader and stronger M2 immunity than live influenza A virus infection. Antivir Res. 2013;99:328–35.
3. Ong HK, Yong CY, Tan WS, Yeap SK, Omar AR, Razak MA et al. An influenza a vaccine based on the extracellular domain of matrix 2 protein protects BALB/C mice against H1N1 and H3N2. Vaccines 2019;7:91.
4. Neirynck S, Dero T, Saelens X, Peter V, Min JW, Walter F. A universal influenza A vaccine based on the extracellular domain of the M2 protein. Nat Med. 1999;5:1157–63.
5. El Bakkouri K, Descamps F, De Filette M, Smet A, Festjens E, Birkett A, et al. Universal vaccine based on ectodomain of matrix protein 2 of Influenza A: Fc receptors and alveolar macrophages mediate protection. J Immunol. 2011;186:1022–31.
6. Schotsaert M, De Filette M, Fiers W, Saelens X. Universal M2 ectodomain-based influenza A vaccines: Preclinical and clinical developments. Expert Rev Vaccin. 2009;8:499–508.
7. Ramos EL, Mitcham JL, Koller TD, Bonavia A, Usner DW, Balaratnam G, et al. Efficacy and safety of treatment with an anti-M2e monoclonal antibody in experimental human influenza. J Infect Dis. 2015;211:1038–44.
8. Mezhenskaya D, Isakova-Sivak I, Rudenko L. M2e-based universal influenza vaccines: A historical overview and new approaches to development. J Biomed Sci. 2019;26:1–15.
9. Orozco S, Oberst A, Program CB, Disease I. RIPK3 in cell death and inflammation: The good, the bad, and the ugly. Immunol Rev. 2017;277:102–12.
10. Nogusa S, Thapa RJ, Dillon CP, Oberst A, Green DR, Nogusa S, et al. RIPK3 activates parallel pathways of MLKL-driven necroptosis and FADD-mediated apoptosis to protect against influenza A virus article RIPK3 activates parallel pathways of MLKL-driven necroptosis and FADD-mediated apoptosis. Cell Host Microbe. 2016;13:13–24.
11. Thapa RJ, Ingram JP, Ragan KB, Nogusa S, Boyd DF, Benitez AA, et al. DAI senses influenza A virus genomic RNA and activates RIPK3-dependent cell death. Cell Host Microbe. 2016;20:674–81.
12. Shubina M, Tummers B, Boyd DF, Zhang T, Yin C, Gautam A et al. Necroptosis restricts influenza A virus as a stand-alone cell death mechanism. J Exp med 2020;217:e20191259.
13. Zheng M, Williams EP, Malireddi RKS, Karki R, Banoth B, Burton A, et al. Impaired NLRP3 inflammasome activation/pyroptosis leads to robust inflammatory cell death via caspase-8/RIPK3 during coronavirus infection. J Biol Chem. 2020;295:14040–52.
14. Oltean T, Van San E, Divert T, Vanden Berghe T, Saelens X, Maelfait J, et al. Viral dosing of influenza A infection reveals involvement of RIPK3 and FADD, but not MLKL. Cell Death Dis. 2021;12:471.
15. Downey J, Pernet E, Allard B, Meunier I, Jaworska J, Qureshi S, et al. RIPK3 interacts with MAVS to regulate type I IFN-mediated immunity to Influenza A virus infection. PLoS Pathog. 2017;3:1–22.
16. Aoshi T, Koyama S, Kobiyama K, Akira S, Ishii KJ. Innate and adaptive immune responses to viral infection and vaccination. Curr Opin Virol. 2011;1:226–32.
17. Sabbaghi A, Miri SM, Keshavarz M, Mahooti M, Zebardast A, Ghaemi A. Role of γδ T cells in controlling viral infections with a focus on influenza virus: Implications for designing novel therapeutic approaches. Virol J. 2020;17:1–18.
18. Kolpe A, Schepens B, Ye L, Staeheli P, Saelens X. Passively transferred M2e-specific monoclonal antibody reduces influenza A virus transmission in mice. Antivir Res. 2018;158:244–54.
19. Chow EJ, Doyle JD, Uyeki TM. Influenza virus-related critical illness: Prevention, diagnosis, treatment. Crit Care. 2019;23:1–11.
20. Longini IM, Halloran ME. Strategy for distribution of influenza vaccine to high-risk groups and children. Am J Epidemiol. 2005;161:303–6.
21. Wu Y, Dong G, Sheng C. Targeting necroptosis in anticancer therapy: Mechanisms and modulators. Acta Pharm Sin B. 2020;10:1601–18.
22. Deroo E, Zhou T, Liu B. The role of RIPK1 and RIPK3 in cardiovascular disease. Int J Mol Sci. 2020;21:1–18.
23. Speir M, Djajawi TM, Conos SA, Tye H, Lawlor KE. Targeting RIP kinases in chronic inflammatory disease. Biomolecules. 2021;11:1–22.
24. Zhang T, Yin C, Boyd DF, Quarato G, Ingram JP, Shubina M, et al. Influenza virus Z-RNAs induce ZBP1-mediated necroptosis. Cell. 2020;180:1115–.e13.
25. Eliasson DG, El Bakkouri K, Schön K, Ramne A, Festjens E, Löwenadler B, et al. CTA1-M2e-DD: A novel mucosal adjuvant targeted influenza vaccine. Vaccine. 2008;26:1243–52.
26. Zebedee SL, Lamb RA. Influenza A virus M2 protein: Monoclonal antibody restriction of virus growth and detection of M2 in virions. J Virol. 1988;62:2762–72.
27. Iwasaki A, Pillai PS. Innate immunity to influenza virus infection. Nat Rev Immunol. 2014;71:233–6.
28. Hänggi K, Vasilikos L, Valls A, Yerbes R, Knop J, Spilgies LM, et al. RIPK1/RIPK3 promotes vascular permeability to allow tumor cell extravasation independent of its necroptotic function. Cell Death Dis. 2017;8:e2588.
29. Salazar G, Zhang N, Fu TM, An Z. Antibody therapies for the prevention and treatment of viral infections. NPJ Vaccines. 2017;2:1–12.
30. Corti D, Cameroni E, Guarino B, Nicole L, Zhu Q, Lanzavecchia A. Tackling influenza with broadly neutralizing antibodies. Curr Opin Virol. 2017;24:60–69.
31. Hughes K, Middleton DB, Nowalk MP, Balasubramani GK, Martin ET, Gaglani M, et al. Effectiveness of influenza vaccine for preventing laboratory-confirmed influenza hospitalizations in immunocompromised adults. Clin Infect Dis. 2021;15213:1–8.
32. Ibañez LI, Roose K, De Filette M, Schotsaert M, De Sloovere J, Roels S, et al. M2e-displaying virus-like particles with associated RNA promote T helper 1 type adaptive immunity against influenza A. PLoS One. 2013;8:e59081.
33. Ramakrishnan MA. Determination of 50% endpoint titer using a simple formula. World J Virol. 2016;6:27–28.
34. Schepens B, Sedeyn K, Vande Ginste L, De Baets S, Schotsaert M, Roose K, et al. Protection and mechanism of action of a novel human respiratory syncytial virus vaccine candidate based on the extracellular domain of small hydrophobic protein. EMBO Mol Med. 2014;6:1436–54.
35. Cho KJ, Schepens B, Seok H, Kim S, Roose K, Lee J, et al. Structure of the extracellular domain of matrix protein 2 of influenza A virus in complex with a protective monoclonal antibody. J Virol. 2015;89:3700–11.

ACKNOWLEDGEMENTS

Our special thanks go to Prof. Saelens's team, in particular Anouk Smet. We thank the VIB Flow Core, the VIB Animal Core Facilities as well as the Bio Imaging Core of Inflammation Research Center (VIB) in particular, Gert Van Isterdael, Kelly Lemeire, Amanda Gonçalves and Benjamin Pavie for their assistance and help. We are grateful to Vishva Dixit (Genentech, Inc., South San Francisco, CA, United States) for providing the *Ripk3*$^{-/-}$ genetically modified mice and to Eik Hofmann and Kristen Penberthy for sharing their expertize and technical knowledge on ADCP experiments and efferocytosis respectively. TO holds a doctoral fellowship from FWO (Flanders Research Organization). NT is paid by Methusalem. Research in the Vandenabeele group is supported by EOS MODEL-IDI (30826052), EOS-INFLADIS (40007512), FWO research grants (G.0E04.16N, G.0C76.18N, G.0B71.18N, G.0B96.20N, G.0A93.22N), Methusalem (BOF16/MET_V/007), iBOF20/IBF/039 ATLANTIS, Foundation against Cancer (FAF-F/2016/865, F/2020/1505), CRIG and GIGG consortia, and VIB. The authors received no specific funding for this work.

AUTHOR CONTRIBUTIONS

NT, XS, and PV designed the study. TO, NT, LI, MS, TD, and TY performed experiments. TO, NT, PV, and XS analyzed the results. VG helped setting-up and analysis of the ADCP experiments. HV and KB helped with the scoring of lung inflammatory profile. TO and PV wrote the manuscript. TO and NT made the figures. PV, NT, JM, XS, and BS revised the manuscript. All authors have read and approved the manuscript.

COMPETING INTERESTS

The authors declare no competing interests.

ETHICS

All animal experiments were performed under conditions specified by law (European Directive and Belgian Royal Decree of November 14, 1993) and reviewed and approved by the Institutional Ethics Committee on Experimental Animals (EC2016-17). The in vivo studies were performed in accordance with the declaration of Helsinki.

ADDITIONAL INFORMATION

Supplementary information The online version contains supplementary material available at https://doi.org/10.1038/s41419-022-04710-2.

Correspondence and requests for materials should be addressed to Peter Vandenabeele.

Reprints and permission information is available at http://www.nature.com/reprints

Publisher's note Springer Nature remains neutral with regard to jurisdictional claims in published maps and institutional affiliations.